Nonlinear Transformer Model for Circuit Simulation

John H. Chan, *Member, IEEE*, Andrei Vladimirescu, *Member, IEEE*, Xiao-Chun Gao, *Member, IEEE*, Peter Liebmann, and John Valainis, *Member, IEEE*

Abstract—A transformer model which consists of a nonlinear core with hysteresis and multiple windings is described as implemented in DSPICE, Daisy's proprietary version of the popular circuit simulator SPICE. The analytical formulation of the major and minor loops, and, the transition algorithm between hysteresis loops is described. The modeling of losses, and frequency and temperature dependence is also presented.

I. INTRODUCTION

TRANSFORMERS differ from the ideal inductors supported by SPICE2 [1] due to the power loss incurred each cycle. An important loss factor is the hysteretic behavior of the flux density and magnetic field in the magnetic core. This paper presents an original approach of modeling a magnetic core in a circuit simulator and its implementation in DSPICE [2].

The addition of a nonlinear magnetic core model has been reported for several commercial versions of the SPICE simulator. The first reported magnetic model implementation [3] emphasizes the correctness of the hysteresis shape and partitions the loop in several regions. A disadvantage of the multiregion analytic description is the introduction of discontinuities at the transition points which have a negative impact on convergence. While SpicePlus [4] uses a multiregion formulation similar to Nitzan's, the magnetic model of PSpice [5] is based on the mathematical formulation reported by Jiles and Atherton [6]. The complexity of the latter makes it difficult to specify the core parameters for a desired hysteresis shape. IG-Spice [7] has also been reported to offer a magnetic model.

In contrast to previous implementations the nonlinear behavior of the new model is described by continuous piecewise-hyperbolic functions characterized by three parameters. These parameters are the same as the parameters published in catalogs of magnetic materials. A loop-traversing algorithm has been implemented which avoids discontinuities and eliminates both nonconvergence problems and the occurrence of erroneous voltage spikes during time-domain simulation. Both the functional representation of the loops and the traversing algorithm minimize the danger of nonconvergence which is apparent in previous models. The details of the hysteresis modeling are included in Section III.

The different effects included in the transformer model are presented in Section IV. In the large signal time-domain analysis the frequency dependent Eddy current losses in the core

and wire losses are modeled. Additional effects such as wire skin effect and temperature dependence are also included. In the small signal ac analysis the transformer is modeled as frequency dependent lossy mutual inductors. For both analyses, air gap and the related fringe field effect are modeled by extending the magnetic path length of the core appropriately. In the transformer model library [8] parasitic capacitances and leakage inductances are added to the core and windings of the transformer.

The last section presents the simulation of a power circuit using the new transformer model. This example shows the accuracy of the new model as well as its usefulness in power circuit design.

II. BASIC MAGNETICS

The branch equation of an inductor is

$$V = \frac{d\phi}{dt} \tag{1}$$

where V is the voltage in volts, and, ϕ is the magnetic flux in Webers.

In the case of a coil, or inductor, with no magnetic material, the flux induced by the flow of current in the windings can be equated to the latter by a proportionality constant L

$$\phi = LI \tag{2}$$

where L is the inductance of the coil in Henries while I is the current in amperes. The inductance is a function of the geometry of the coil and the number of windings, and is independent of the current. Equations (1) and (2) describe the linear inductor supported in SPICE 2G6 [9].

In the case of a transformer where the windings surround a magnetic material, the core, the relation between the flux and current is no longer linear. Two additional magnetic quantities, the magnetic field, H, induced in the core, and the magnetic induction or flux density, B, must be computed. The magnetic field in the core is obtained by summing up the contributions H_i of each winding:

$$H = \sum_{i=1}^{n} \frac{\kappa_i N_i I_i}{l_{\text{mag}}} \tag{3}$$

where N_i is the number of turns in winding i, $0 \leq \kappa_i \leq 1$ is the coupling of the winding to the core, I_i is the current through winding i, and l_{mag} is the effective magnetic path length of the core. In the above equation H is expressed in (ampere-turns/meters), the International System unit. The flux density, B, can be equated to the magnetic field, H, by the permeability, $\mu = \mu_r \mu_0$, of the magnetic material

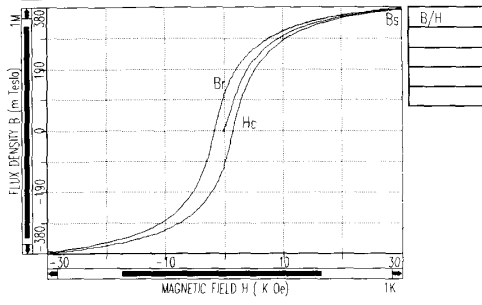$$B = \mu_r \mu_0 H = \frac{\phi}{A}. \tag{4}$$

Fig. 1. Major magnetic hysteresis loop.

The above equation is valid only in the International System, where μ_0, the permeability of free space, is $4\pi \times 10^{-7}$ H/m; μ_r is the relative permeability of the material and is a function of H, H is measured in ampere-turns/meters, 1 A-turn/m = $4\pi 10^{-3}$Oe, A is the cross-sectional area in square meters, and B is the flux density in Tesla, 1 T = 10^4 G.

Furthermore, B is not only a nonlinear function of H, but depends on the history of the magnetic fields applied to the core:

$$B = B(H, \text{history}). \tag{5}$$

The result is a hysteresis curve in the B-H plane as shown in Fig. 1. These curves are the result of applying a sinusoidal current to a winding of a transformer and are studied in more detail in the following section. The amplitude of the current and the number of turns is chosen such that the field H, computed according to (3), is large enough to saturate the core.

The nonlinearity introduced by (4) can significantly change the circuit behavior compared to the linear case of (2). The voltage across a winding of the transformer results by solving (1), (3), and (4). The solution of these history-dependent time-varying nonlinear functions using the SPICE algorithms constitutes the major difficulty of the nonlinear core model implementation.

In circuit design it is often necessary to estimate the impedance of the windings of a transformer. For this purpose it is useful to define an equivalent inductance based on substitution of (3) and (4) in (2):

$$L_{eq} = \frac{4\pi 10^{-7} \mu_r(H) N^2 A}{l} \tag{6}$$

where L_{eq} is expressed in Henries, A in square meters, l in meters, and μ_r is averaged over the operating region of the core.

III. Hysteresis Modeling

A major hysteresis loop, shown in Fig. 1, is characterized by three parameters, H_c, B_r, and B_s. H_c, known as the coercive force, is given by the intersection of the major loop with the positive H axis. B_r, the remnant flux, is the intersection of the major loop with the positive B' axis. The limit of the magnetic flux density B when H increases is

$$\lim_{H \to \infty} B = \mu_0 H + B_s \tag{7}$$

which defines the saturation flux, B_s. For most fields encountered in practice the $\mu_0 H$ term is small compared to B_s. The major loop represents the envelope of all B-H curves and is attained when the current through the windings is large enough to saturate the core.

Several approaches to model the hysteresis curves of magnetic cores have been reported [3], [10]. Two hyperbolic curves have been found to fit well the experimental data measured for ferrites [11]. In our model the major loop is composed of two branches: a lower branch which applies for increasing fields H and an upper branch which applies for decreasing fields. The branch equations are defined below in terms of the flux $B' = B - \mu_0 H$.

The upper branch is given by:

$$B'_+(H) = B_s \frac{(H + H_c)}{|H + H_c| + H_c\left(\frac{B_s}{B_r} - 1\right)}. \tag{8a}$$

The lower branch is given by:

$$B'_-(H) = B_s \frac{(H - H_c)}{|H - H_c| + H_c\left(\frac{B_s}{B_r} - 1\right)}. \tag{8b}$$

Notice that we have inversion symmetry through the origin of the B', H plane. That is

$$B'_+(H) = -B'_-(-H). \tag{9}$$

The magnetization curve is the path in the H, B' plane which is followed if we start at $H = 0$, $B' = 0$, and increase or decrease the field without reversals. In the present model the magnetization curve is given by the average of the upper and lower branches of the major loop. Specifically:

$$B'_{mag}(H) = \frac{B'_+(H) + B'_-(H)}{2}. \tag{10}$$

Next we discuss the normal minor loops. These are the loops which are followed if H varies periodically from some $-H_{max}$ to H_{max} and back without any reversals of the direction of change of H except at the end points of the interval. The values of B' at the end points are denoted by $-B_{max}$ and B_{max}. The points $(-H_{max}, -B_{max})$ and (H_{max}, B_{max}) are called the extreme points of the minor loop.

In the current model the lower branch of a minor loop is obtained by translating the lower branch of the major loop vertically upward by some amount B_d where $0 \le B_d \le B_r$. The upper branch of the minor loop is obtained by translating the upper branch of the major loop downward by the same amount B_d. The intersection points of the upper and lower branches of the minor loop will lie on the magnetization curve $B_{mag}(H)$. These intersection points are just the extreme points of the minor loop.

The equations for a minor loop with a given value of B_d are

$$\text{upper branch: } B'(H) = B'_+(H) - B_d \tag{11a}$$

$$\text{lower branch: } B'(H) = B'_-(H) + B_d. \tag{11b}$$

Let us see how we move around in the (H, B') plane during a simulation. (Note that we always stay within the major loop.)

If we start from $H = 0$, $B' = 0$, represented by point A in Fig. 2, and increase H, we move along the magnetization curve, curve AFB in Fig. 2. Suppose that when H reaches 4 A-turns/m we begin to decrease H. We now move onto the upper branch of the minor loop at the upper extreme point which is located at the place where H begins to decrease, point B in Fig. 2. If H now decreases to exactly $-H_{max}$, $H_{max} = 4$ in our example, and then starts to increase again, we move onto the lower branch of
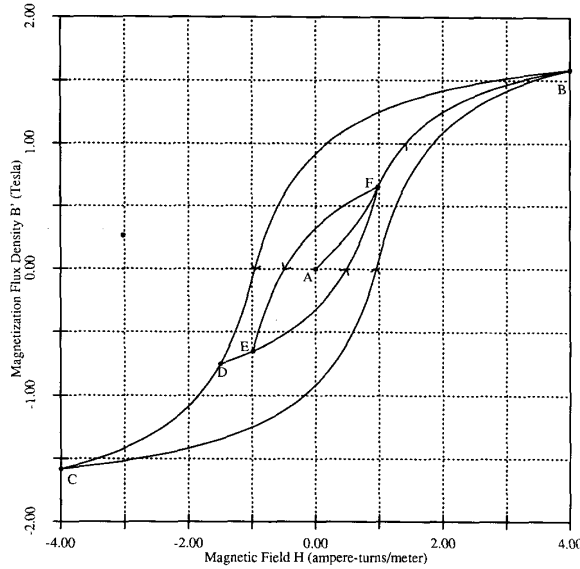
Fig. 2. Minor loops and magnetization curve (Case 1).

Fig. 3. Minor loop generation in Case 2.

the same minor loop. If we now continue to move periodically between $-H_{max}$ and H_{max} with no reversals in between, then we will stay on the same minor loop.

If we are moving along a minor loop and arrive at an extreme point but do not reverse the direction of change of H then we will move onto the magnetization curve again. Also note that each branch of a minor loop has a proper direction of motion. If we are on the lower branch then H must be increasing while on the upper branch H must be decreasing.

Next suppose that we are on a minor loop and reverse the direction of H at a point which is not an extreme point. Assume that we are moving along the upper branch of the outer minor loop shown in Fig. 2. We arrive at point D and H starts to increase. There are then two cases to be considered.

Case 1: As shown in the figure there is an extension of the lower branch of a valid minor loop, with $0 \le B_d \le B_r$, which passes through point D. In this case we follow the extension. This extension is given by the same analytical form as the lower branch of the minor loop but we have $H < -H_{max}$. For the main body of the minor loop we had the restriction $-H_{max} \le H \le H_{max}$. The valid minor loop has the extreme points E and F.

Case 2: The point where H changes direction does not lie on the extension of a normal minor loop with the proper direction of motion. This is the case when $B_d > B_r$. When $B_d = B_r$ the corresponding minor loop is a point at the origin; for larger values of B_d no minor loops exist. In Fig. 3 the dotted curve starting from point B is the vertical translate exactly by B_r of the lower branch of the major hysteresis loop. Thus there is no extension of a lower branch of a normal minor loop to follow when a reversal of the field occurs at points on the upper branch of the minor loop between B and C.

In this case the model uses a path constructed as follows. Suppose that we are at point D (between B and C) in Fig. 3 and H is increasing. We use a path which is a translate of the lower branch of the minor loop that D is on, defined by the extreme points A and C. We translate the lower branch of the minor loop in such a way that its lower extreme point A is trans-
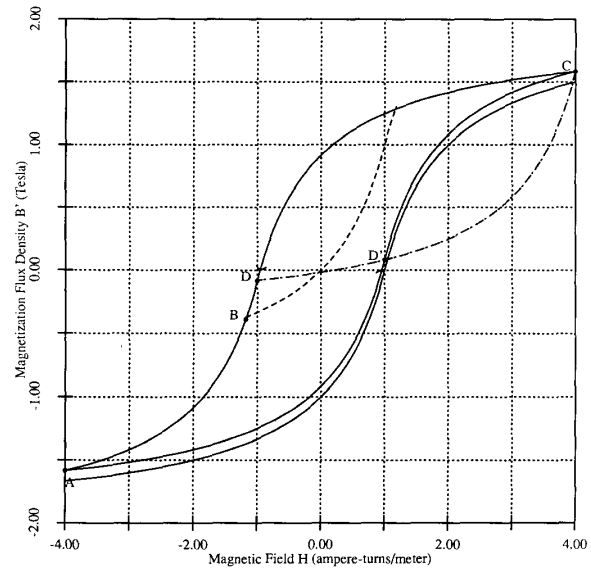
lated to D. Let the coordinates of D be (H_D, B'_D). Then we note that because of the symmetry of the hysteresis loops, the point D' with coordinates $(-H_D, -B'_D)$ is on the lower branch of the same hysteresis loop that D is on. The extreme point $(-H_{max}, -B'_{max})$ is translated to D. Thus the translation vector is given by

$$(\Delta H, \Delta B') = (H_D + H_{max}, B'_D + B'_{max}). \qquad (12)$$

The translate of D' is thus

$$(-H_D, -B'_D) + (\Delta H, \Delta B') = (H_{max}, B'_{max}) \qquad (13)$$

which is the upper extreme point of the minor loop. Thus the translated lower branch intersects the upper branch of the minor loop at D and at its upper extreme point, C. This translated lower branch is the curve that we leave D on for increasing H and follow until H begins to decrease again or until we come to the upper extreme point.

If point D had been on a lower branch with H initially increasing but changing to decreasing at D, then the above discussion still holds with upper and lower, increasing and decreasing interchanged everywhere.

IV. Transformer Model

A. Windings, Cores, and Parasitics

Fig. 4 shows the equivalent model of a transformer including parasitics. The main component of a transformer is the magnetic core which has two or more windings. A basic transformer, e.g., TRF3 in Fig. 4, has a core, $B1$, and two or more windings, e.g., $Y1$, $Y2$, and $Y3$.

The core element statement contains such information as number of windings, magnetic length LM, cross-sectional area A, air gap LG, window height G, the frequency of signals, and the magnetization at time 0. Each core statement also contains the name of a core model. The core model statement defines B_r, B_s, and H_c and all coefficients of the modeled effects which are listed below. Each winding Y statement defines the number of

L1,L2: Leakage inductance;
R1,R2: Wire resistance;
C1,C2: Winding capacitance;

N1,N2: number of turns of windings 1 and 2;
K1,K2: Coupling coefficients;

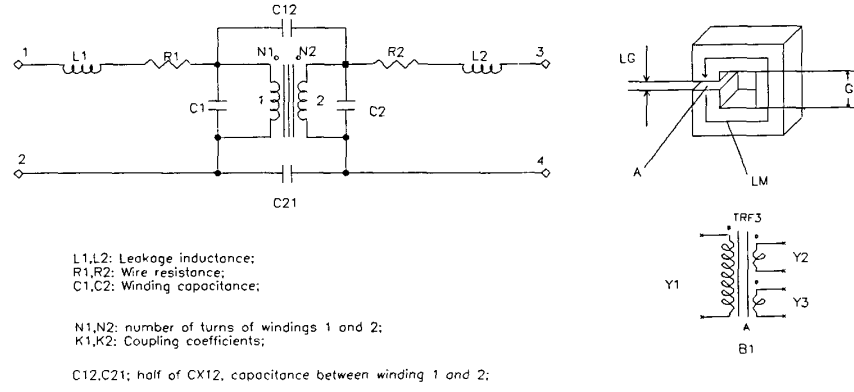C12,C21; half of CX12, capacitance between winding 1 and 2;

Fig. 4. Transformer equivalent model.

turns, the coupling coefficient, the name of the core it is wound on, and the initial current through the winding.

For a real transformer there are parasitic components associated with the main inductors and mutual inductances. Each winding has capacitances between turns of the winding. They are represented by $C1$ and $C2$ in Fig. 4 for a two winding transformer TRF1. $C12$ is the interwinding capacitance. The wire resistance is frequency dependent, and will be discussed later. The leakage inductance, which accounts for the flux that does not go through the magnetic core, and therefore, does not contribute to the mutual inductance, is separated out as $L1$ and $L2$ in Fig. 4. If the inductances of the two transformer windings are $Y1$ and $Y2$, then the coupling coefficient K for the mutual inductance between the two windings is

$$K = \sqrt{\frac{Y1\,Y2}{(Y1 + L1)(Y2 + L2)}}. \tag{14}$$

B. Frequency Behavior

The area enclosed by the hysteresis loop represents the energy loss to the core due to the irreversible movement of the magnetic domains in the core material and the Eddy current ohmic loss [6]. The energy loss to the core has a very pronounced frequency dependence. This dependency is modeled by modifying the effective H_c:

$$H'_c = H_c(f_1 + f_2 f^{f_3}) \tag{15}$$

where f is the operating frequency and f_1, f_2, f_3 are three empirical coefficients.

H_c increases with frequency and consequently the hysteresis loop widens. Therefore, the higher the frequency the more energy is dissipated due to core loss. The coefficients f_1, f_2, and f_3 are obtained by curve fitting the loss curves of core materials from data sheets. f_1 is usually 1.0 and f_3 is about 2.0. Since this is an empirical equation fitted to real loss data, all kinds of microscopic losses by the core are taken care of, such as the Eddy current loss.

Additional power loss is due to the ohmic loss of the windings. This wire loss is also frequency dependent due to the skin effect. The winding parasitic resistance is modified as

$$R'_w = R_w \frac{r^2}{r^2 - \left(r - \frac{504}{\sqrt{\sigma \mu_r f}}\right)^2} \tag{16}$$

where R_w is the resistance of the winding in ohms, r is the radius of the wire in meters, and σ is the conductivity of the wire in mho.

C. Temperature Behavior

The temperature dependence is modeled by a linear variation of the three basic parameters B_s, B_r, and H_c with temperature T. The temperature variation of the saturation flux density is expressed as

$$B'_s = B_s(1 + (T - T_{nom})TBS) \tag{17}$$

where T_{nom} is a reference temperature and TBS is the temperature coefficient for B_s. There are similar relations for B_r and H_c.

D. Air Gap

The air gap in the core can drastically change the shape of the hysteresis loop. A minute gap introduced into the core can prevent the core from saturating. The reason for this is that the permeability of air is so much smaller than that of the magnetic core material. The air gap effectively lengthens the magnetic path of the core:

$$L'_m = L_m + \mu_r L_g \tag{18}$$

where L_g is the length of the air gap.

However, the lengthening effect is not as large as indicated in (18) due to the fringe fields at the gap. An approximation for the fringe field effect [12] is to modify the above equation to
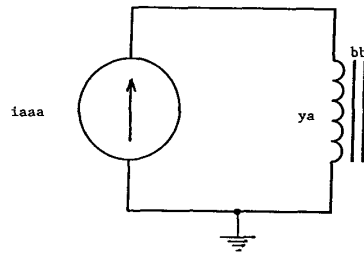
$$L'_m = \frac{L_m + \mu_r L_g}{1 + \frac{L_g}{\sqrt{A}} \ln\left(\frac{2G}{L_g}\right)} \tag{19}$$

where A is the cross-sectional area of the core and G is the window height of the core gap, as shown in Fig. 4.

E. Inrush Current

A high current may flow in a transformer winding upon initial connection to a sinusoidal voltage source. This potentially high current, termed inrush current [13], is a function of the phase shift of the sinusoidal source at time 0. The inrush current can be specified for each winding as an initial condition.

Often the core retains a residual magnetization. This magnetization can affect the turn-on behavior of the circuit by add-
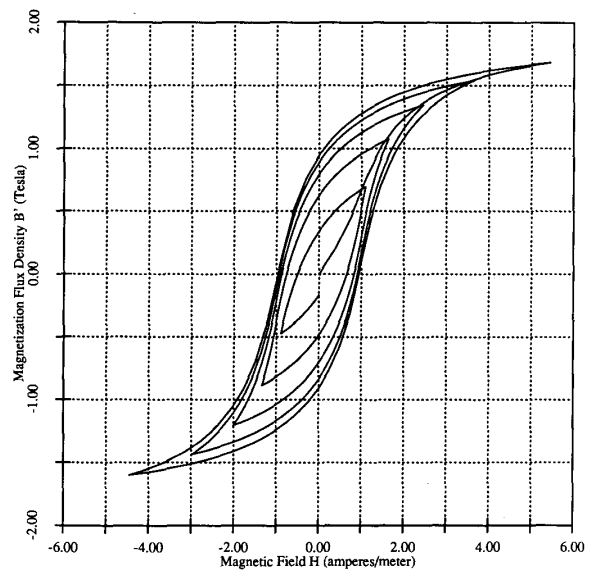
transformer test
.model core1 tfm bs = 2.0 br = 1.0; hc = 1.0 fc1 = 1.0 fc2 = 0.0
+ fc3 = 0.0 tbs = 0.0 tbr = 0.0 thc = 0.0
iaaa 0 1 sin(0.0 6.0 1e3 0.0 .4e3)
vaaa 1 2 0.0
ya 2 0 bb 1 1.0
bb 1 core1 lm = 1.0 a=1.0 lg=0.0
.tran .01 10.0 0.0 0.01
.print tran i(vaaa) b(bb)
.options limpts = 10000
.end

Fig. 5. Single-winding transformer circuit and DSPICE netlist.

Fig. 6. (H, B') plane loops of single-winding transformer. Circuit for damped sinusoidal input.

ing another component to the inrush current. An initial flux density B_0 can be specified for each core in the circuit. B_0 together with the H determined from the initial currents establish the exact state of the transformer at time 0. The initial state of the transformer can be specified to be anywhere within the major loop of the core.

V. RESULTS

Numerous circuits with magnetic core transformers have been simulated using DSPICE. These simulations using the transformer model described above have produced accurate results and have not caused convergence problems. The simulations of two magnetic circuits are presented below along with comments on the accuracy of the magnetic modeling.

The correctness of the model can be judged first for a simple one-winding transformer driven by a damped sine wave current source. The circuit is shown together with a SPICE netlist in Fig. 5. The hysteresis loops plotted in Fig. 6 show the smooth transition from one minor loop to another with no breaks or discontinuities.

A more representative circuit for the applications of a transformer model is a square wave power oscillator converter, also referred to as a Royer oscillator [14]. The circuit schematic is presented in Fig. 7. The heart of the circuit is the square hysteresis loop of the transformer core $B1$. The transformer core has five windings $Y1$ through $Y5$ with the specified polarity.

The circuit operates between two states. First assume that transistor $Q1$ is saturated and thus its collector, node 3, is at V_{cesat} (see Fig. 8). The saturation current flowing through $Y1$ produces, through inductive coupling, a voltage drop

$$V_{Y4} = \frac{n_4}{n_1} V_{Y1} \tag{20}$$

across $Y4$ which drives the base of $Q1$ positive and keeps $Q1$ in saturation. Due to the reverse polarity of $Y3$ the base of $Q2$ is driven negative and $Q2$ is turned off. Fig. 8 displays the plots
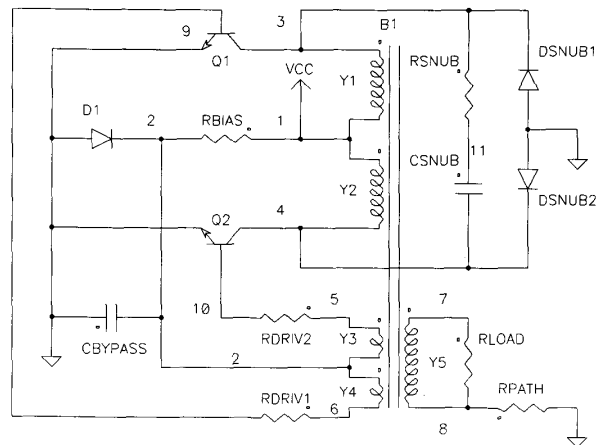

Fig. 7. Square wave power oscillator.

of the collector voltages of $Q1$ and $Q2$ as well as the flux density of the magnetic core versus time. The oscillation is centered around $V_{cc} = 12$ V with the collector of $Q1$ at V_{cesat} and the collector of $Q2$ at $2V_{cc} - V_{cesat}$. During the time that saturation current flows through $Q1$ the magnetic flux density in $B1$ decreases linearly with time because the voltage drop across $Y1$ is constant:

$$\frac{dB}{dt} = \frac{V_{Y1}}{n_1 A} = \frac{V_{cc} - V_{cesat}}{n_1 A} \tag{21}$$

Fig. 9 shows the plot of flux density in the (H, B') plane. B decreases linearly with time, as seen in Fig. 8, until it reaches the saturation value $-B_s$. At this point B cannot decrease any further and V_{Y1} falls to zero; this pulls the collector of $Q1$ to the supply V_{cc}. The current diverted through $R1$ flows partly in the base of $Q2$, turns it partially on, and generates a positive
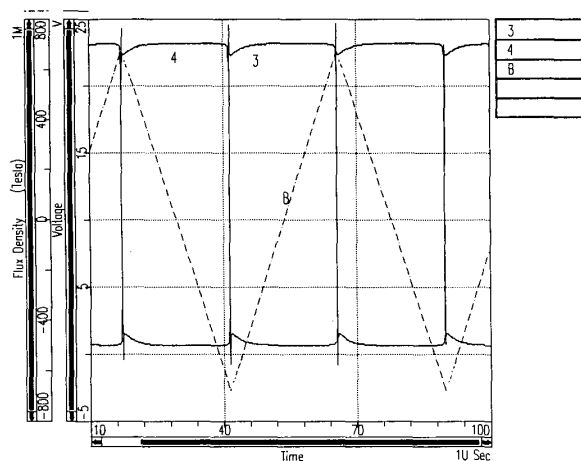
Fig. 8. Collector voltages of transistors $Q1$ and $Q2$, and magnetic flux density through core $B1$.
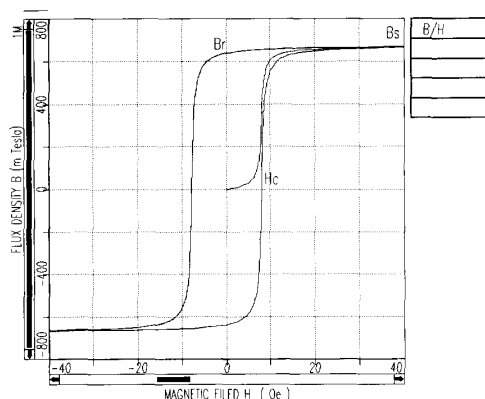

Fig. 9. (H, B') plane hysteresis loops of $B1$ during oscillations.

magnetic field in the core. A positive feedback effect leads to the saturation of $Q2$ and the cutoff of $Q1$. At the same time B increases at a constant slope toward B_s. When it reaches that point the circuit switches and the process continues periodically. The waveforms in Figs. 8 and 9 produced by DSPICE demonstrate the correct simulation of the Royer oscillator. The period of oscillation can be derived from (21) and is in agreement with the simulation results of Fig. 8:

$$T = \frac{4B_s n_1 A}{V_{cc} - V_{cesat}} = 45 \ \mu s \qquad (22)$$

for a magnetic core with $B_s = 0.675$ T, a cross section area $A = .05$ cm^2, and 40 turns in the winding $Y1$. The supply voltage $V_{cc} = 12$ V.

VI. CONCLUSIONS

An extension of the applicability of SPICE2 to the systems and power electronics field has been described. The simulation capabilities are extended in DSPICE by supporting a transformer representation and a nonlinear magnetic core model.

Three new statements are used to specify a transformer in DSPICE: a core statement contains geometry information and

the name of a core model, a model statement specifies the core hysteresis characteristics and coefficients for various effects, and, finally a winding statement defines the characteristics of each winding.

The most complex issue of the transformer implementation, the support of a nonlinear history dependent function in the context of the Newton–Raphson algorithm, has been presented in detail. The correctness of the algorithm has been verified by the results of a square wave oscillator simulation.

ACKNOWLEDGMENT

The authors would like to acknowledge the participation through suggestions and discussions of Daisy's technical specialists, application engineers, and DSPICE users.

REFERENCES

[1] L. W. Nagel, "SPICE2: A simulation program with integrated circuit emphasis," ERL Memo ERL-M520, Univ. California, Berkeley, May 1975.
[2] ——, "Analog simulation tools," Daisy Systems Corp., Mountain View, 1988.
[3] D. Nitzan, "MTRAC: Computer program for the transient analysis of circuits including magnetic cores," IEEE Trans. Magn., vol. MAG-5, pp. 524–533, Sept. 1969.
[4] M. Tabrizi, "Nonlinear magnetic model realistically simulates core behavior," Powertech. Mag., Mar. 1988.
[5] ——, "PSpice," MicroSim Corp., Irvine, CA, 1989.
[6] D. C. Jiles and D. L. Atherton, "Theory of ferromagnetic hysteresis," J. Magnet. and Magn. Mater., vol. 61, pp. 48–68, 1986.
[7] J. C. Bowers, "I-G SPICE—A circuit designer's dream," Powerconversion Int., vol. 9, pp. 36–40, June 1983.
[8] ——, "Analog libraries," Daisy Systems Corp., Mountain View, 1988.
[9] A. Vladimirescu, K. Zhang, A. R. Newton, D. O. Pederson, A. Sangiovanni Vincentelli, "SPICE version 2G user's guide," Dept. EECS, Univ. California, Berkeley, 1982.
[10] M. K. El-Sharbiny, "Representation of magnetic characteristics by a sum of exponentials," IEEE Trans. Magn., vol. MAG-9, pp. 60–61, Mar. 1973.
[11] D. R. Bennion, D. C. Hewitt, and D. Nitzan, Digital Magnetic Logic. New York: McGraw-Hill, 1969.
[12] W. T. McLyman, Magnetic Core Selection for Transformers and Inductors. New York: Marcel Dekker, 1982.
[13] S. A. Nasar, and L. E. Unnewehr, Electromechanics and Electric Machines. New York: Wiley, 1983.
[14] A. Pressman, Switching and Linear Power Supply, Power Converter Design. Rochelle Park, NJ: Hayden, 1977.

John Chan (M'84) received the B.A. and Ph.D. degrees in physics from the University of California, Berkeley, in 1970 and 1976, respectively.

He has worked at the Fairchild Research Center, Shiva Corp., and Daisy Systems Corp. on various aspects of analog simulation and device modeling. Currently he is teaching at the University of Hong Kong. His current interests include CAD for VLSI, analog simulation, and parallel algorithms.
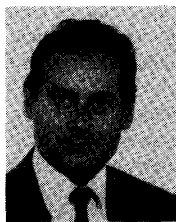
Andrei Vladimirescu (S'79–M'82) received the Diploma Engineering degree in electronics from the Polytechnic Institute in Bucharest, Romania, in 1971, and the M.S. and Ph.D. degrees in electrical engineering and computer sciences from the University of California, Berkeley, in 1980 and 1982, respectively.

From 1971 to 1977 he was with the Research and Development Center for Electronic Components, in Bucharest, Romania, where he worked in the areas of CAD tools and MOS IC design and modeling. In 1977 he joined the IC/CAD research group of the EECS Department, University of California, Berkeley, where he carried out research in the area of electrical simulation, specifically LSI electrical simulation on parallel computers and semiconductor device modeling. In 1983 he joined the Linear Signal-Processing Division of Analog Devices Inc., where he participated in the development of CAD tools for ASIC's, and then from 1984 to 1988 he was Research and Development director of the Analog Division at Daisy Systems Corp., where he led the development of Daisy's analog computer-aided engineering product and the research for a SPICE hardware accelerator. Since 1988, he has been Research and Development Director at Analog Design Tools Inc., and subsequently at Valid Logic Systems Inc. His current research interests are in the areas of computer simulation, including algorithmic issues, component and higher level modeling, analog hardware description languages, and mixed analog–digital and electrical–physical design tools.

Xiao-Chun Gao (M'88), photograph and biography not available at time of publication.
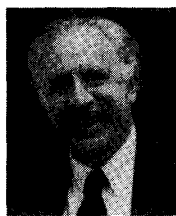
Peter Liebmann received the B.A. degree in mathematics from Clark University, and the Ph.D. degree in physical chemistry from New York University, in 1969.

From 1969 to 1980 he held research grants at various universities where he developed numerical techniques to facilitate the understanding of a variety of problems related to molecular biology, surface physics, and other quantum-chemical phenomena. He is presently Project Development Manager at Electrical Engineering Software, Santa Clara, CA. Before EES he worked at the Fairchild Research Center on the in-house circuit simulator, and afterwards, at Daisy Systems Corp. where he was the main contributor to the DSPICE simulation program.

John Valainis (M'90) received the B.S. degree in physics from Butler University, Indianapolis, IN, and the M.S. and Ph.D. degrees in physics from the California Institute of Technology, in 1975 and 1982, respectively.

He has been employed by Schlumberger Research Center, Palo Alto, CA, and Daisy/Cadnetix, Mountain View, CA. He is currently with Valid Logic Systems, San Jose, CA. His interests include CAD for VLSI, analog simulation, electromagnetic problems, and various aspects of physics.